

GaN: FROM SELECTIVE AREA TO EPITAXIAL LATERAL OVERGROWTH

X. Li, S. G. Bishop and J. J. Coleman

University of Illinois, Urbana, IL 61801

Cite this article as: **MRS Internet J. Nitride Semicond. Res. 4S1, G4.8 (1999)**

ABSTRACT

The evolution of the topography of GaN stripes as a function of stripe width (2 – 120 μm), fill factor and substrate smoothness has been explored. The spatially resolved optical properties of these structures have been characterized by cathodoluminescence imaging and line scans. Implications from the optical study have been discussed.

INTRODUCTION

Epitaxial lateral overgrowth (ELO) of GaN on patterned substrates has been widely studied since the realization of a long lifetime GaN-based laser diode (LD) using this technique.¹ It is believed that ELO reduces dislocation density by blocking the dislocation propagation from the under layer using the oxide mask. Using ELO to reduce dislocation density on mismatched heteroepitaxial semiconductor layers can be dated back to the extensive study of ELO by liquid phase epitaxy (LPE) by Nishinaga *et al.*² It has been demonstrated by many groups that the application of this technique leads to the growth of extremely low dislocation density materials including GaAs, InP, $\text{Ge}_x\text{Si}_{1-x}$ on Si substrates and InGaAs on a GaAs substrate. In addition, the ELO technique is useful to relieve stress caused by both the lattice mismatch and the difference in thermal expansion coefficient.³

An ELO process starts from a basic selective area epitaxial (SAE) substrate which is usually patterned lithographically with a dielectric material such SiO_2 or SiN_x as the mask. In the ideal SAE case, deposition can only take place within the openings but not on the mask. However, lateral growth on top of the mask beyond the opening is possible. Illustrated in Figure 1 (cross-section view) are three possible types of sidewall growth topographies for stripe patterns. In the case of Figure 1(a), there is zero tendency for lateral growth and a rectangular cross section with the same width as the mask opening is obtained. GaN rectangular shaped waveguides and GaN hexagonal micropisms with smooth vertical facets have been fabricated.^{4,5} In the case of a nonzero ratio of lateral-to-vertical growth rate, which depends on the mask pattern and the growth conditions, growth beyond the opening can be obtained (Figure 1(b)). Kopolnek *et al.* have reported anisotropy in GaN epitaxial lateral growth.⁶ Prolonged growth leads to the coalescence of adjacent selectively grown stripes and a flat surface across the entire substrate, as demonstrated by Nam *et al.* for GaN growth using SiC substrates.⁷ Figure 1(c) shows another type of topography where the vertical growth planes face out as growth proceeds and a triangular cross section is developed. For GaN selective growth on a 10 μm wide stripe, Kato *et al.* identified the side facets of the triangle as (1101).⁸ Prolonged growth in this case also leads to the coalescence of the selectively grown stripes by growing on the side facets of the triangle, and eventually the top surface will level off. Usui *et al.* have recently demonstrated the growth of a continuous thick GaN film with low dislocation density by hydride vapor face epitaxy (HVPE) from the coalescence of (1101) facets on the oxide mask.⁹ We have previously reported the selective growth of GaN by atmospheric pressure MOCVD, with focus on the topography and optical properties of the wide stripes (50 - 125 μm).¹⁰ Recently, we have also demonstrated the ELO of GaN from narrow stripes (2 – 6 μm) with triangular cross sections and

explored the spatially resolved optical properties at each ELO stage.¹¹ In this paper, we explore the evolution of topography of GaN structures grown by SAE and subsequent ELO as a function of pattern geometry and growth parameters. We also discuss the origin of different emission bands of GaN through spatially resolved cathodoluminescence study.

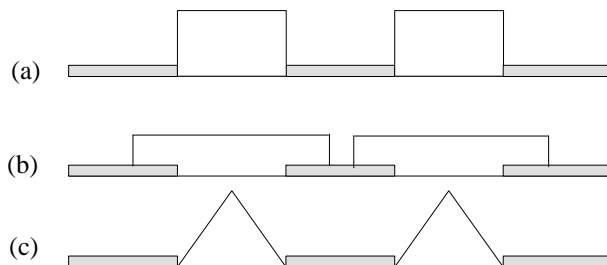


Figure 1 A schematic of three types of growth topography (cross section) for stripe patterns (a) SAE with vertical sidewalls. (b) ELO with vertical sidewalls (c) SAE with triangular cross section.

EXPERIMENTAL

The GaN growth was carried out in a vertical configuration atmospheric pressure MOCVD reactor. TMGa and NH₃ were used as Ga and N precursors, respectively. H₂ was used as a carrier gas. A buffer layer grown at ~ 550°C was deposited on (0001) sapphire substrate before the growth of GaN epi-layer. Lithographically defined patterns were formed either on a 3 μm thick GaN epilayer or directly on a GaN buffer layer. Patterns studied include stripes (50 – 120 μm) spaced by 350 μm, arrays of narrow stripes (2– 6 μm wide) spaced by 2 – 10 μm between stripes and by 350 μm between stripe arrays. A cross structure (25 x 80 μm) is also studied in this report. The stripes were oriented either perpendicular or parallel to the sapphire (11 $\bar{2}$ 0) flat. Under our typical growth condition, the lateral growth rate for these two directions differ by a factor of 1.5. The patterned samples were then heated under NH₃ in the MOCVD chamber to ~1020°C for the growth of the GaN overlayer. A Zeiss SEM equipped with Oxford MonoCL setup was used for morphology and optical characterization. All cathodoluminescence (CL) spectra and images were taken at room temperature. A DI nanoscope III AFM was used for topography measurements. Details of the growth condition and the CL setup have been described previously.^{10,12}

RESULTS AND DISCUSSION

1. Topography Evolution

1.1 Topography Evolution with stripe width

We have grown GaN wide stripes (25 – 120 μm) spaced by 350 μm on a 3 μm thick GaN epilayer. Figure 2 shows an AFM image of a 75 μm wide stripe. Growth rate enhancement is a common phenomenon in selective area epitaxy, due to the lateral diffusion of source materials from the masked to the open area. The nominal growth thickness in this case is 0.2 μm. The enhancement factor is in the range of 5 – 10 from the stripe center to the edge. Under the specified experimental condition, 5 μm-wide plateaus are observed at the edges. As previously reported, the width of the terraces do not appear to change with stripe width and presumably is limited by the surface diffusion length of the Ga species.¹⁰ Note that wide stripes grown directly

on a low-temperature-grown buffer layer do not form wide plateaus, probably because of the smaller diffusion length due to rough surface.

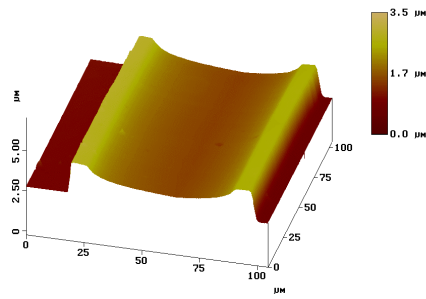


Figure 2 AFM image of a 75 μm GaN stripe grown on a 3 μm GaN epilayer.

Figure 3 shows a SEM image of a cross structure and an AFM image of part of the cross. As in the case of stripes, plateaus are observed at the edges of the cross. The plateau shape is different because the concentration gradient of the source materials, which drives the lateral diffusion, depends on the geometry of the pattern. For stripes, diffusion comes from both sides of the stripe equally. For a cross structure of this width, the lateral diffusion of source materials between the two arms goes to both arms, while the middle of the convex edge of the cross gets enhancement similar to the stripe case. In fact, the width of the plateau at the middle point of the convex edge is about 5 μm , as is the case for the stripes. Note that the rough morphology of the edges in this structure can be improved by increasing the NH_3 flow, as described in the previous paper for the stripes.¹⁰

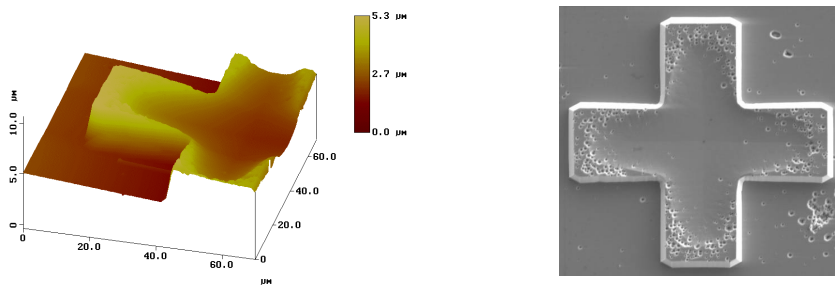


Figure 3 Right: SEM image of a 25 μm cross structure. Left: AFM image of the same structure, partial. The arm width of the cross is 25 μm and the length is 80 μm .

Based on the nature of the plateau, one can speculate that as the stripe width decreases, the stripe should continue having the two plateaus on both sides but the concave profile in the middle should be reduced with stripe width. Furthermore, for stripes narrower than the plateau width (5 μm in this case), the top should be leveled. Figure 4 shows an AFM image of an array of 3.5 μm wide stripes and its cross section. Indeed, these stripes show flat tops and vertical sidewalls. This is the case illustrated in Figure 1(a).

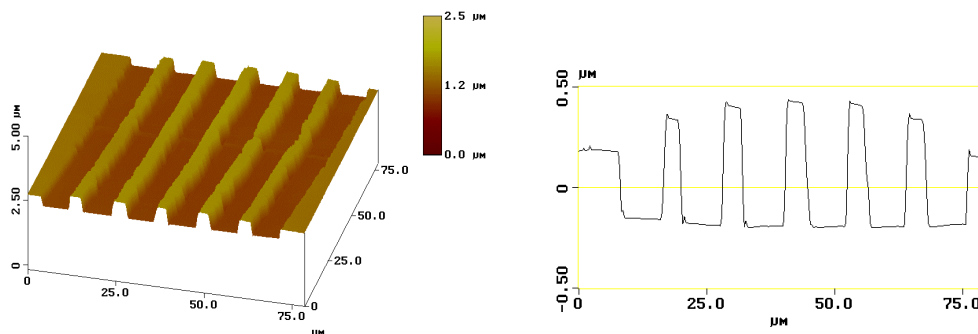


Figure 4 an AFM image of an array of 3.5 μm wide stripes (left) and its cross section (right).

1.2 Topography evolution with growth condition

However, stripes with triangle cross sections, case (c) in Figure 1, can be formed easily. Shown in Figure 5 is an array of 5 μm wide stripes with triangular cross sections. It has been reported that the topography of the stripes depends on pattern orientation and growth parameters such as growth temperature, flow rates and V/III ratios.¹³⁻¹⁵ We report here that two other factors also play a role: fill factor (ratio of open to masked area) and surface roughness. (1) Fill factor effect: a small fill factor (e. g. narrow stripes near a large masked area) favors the formation of triangular cross sections. Smaller fill factor give rise to larger effective flow rate of Ga species due to lateral enhancement from the masked region, and thus smaller surface diffusion length on the (0001) surface. (2) Surface roughness effect: SAE directly on a low-temperature-grown buffer layer (rough) yields triangular stripes while SAE on a high quality GaN epilayer yields rectangular stripes. Rough surface also results in smaller surface diffusion length. The above observation and analysis are consistent with the following picture: the small diffusion length on the (0001) plane makes it a fast and thus invisible growth plane because the adsorbed Ga species do not diffuse to the side walls. Our hypothesis is consistent with that proposed by Nam *et al.* in their study of the effect of Ga flow rate on the stripe morphology.¹⁴

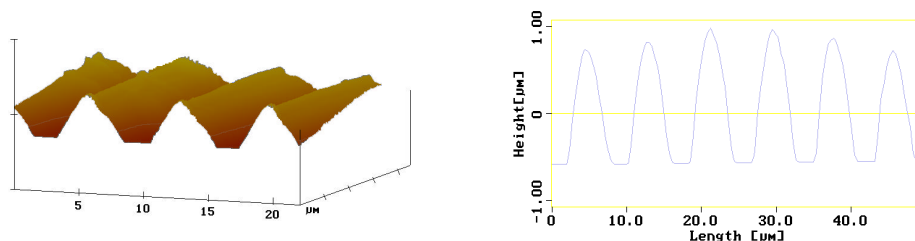


Figure 5 An AFM image of an array of 5 μm wide stripes and its cross section.

Similar to the rectangular shaped stripes, prolonged growth over these triangular stripes also lead to lateral overgrowth on the masked area.^{9,11}

2. Spatially resolved optical characterization

2.1 Reverse contrast between yellow and band-edge emission

It has been proposed that yellow emission originates from threading dislocations and threading dislocations quench band-edge luminescence.^{16,17} Figure 6 and 7 show two cases where precise reverse contrast between the band-edge and yellow emission has been observed in CL imaging.

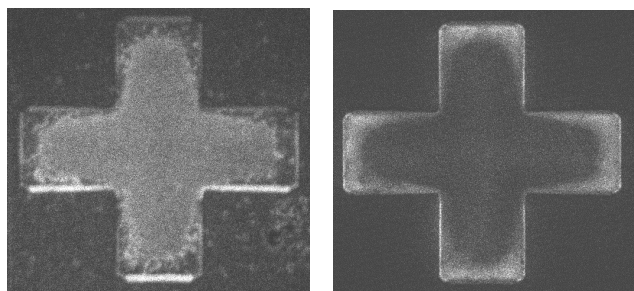


Figure 6 CL images of the cross taken at 360 nm (left) and 560 nm (right). See Figure 3 for the corresponding SEM image.

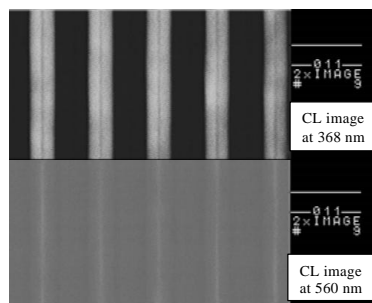


Figure 7 CL images of an array of triangular stripes with 3.7 μm opening and 5 μm spacing taken at 368 nm (upper) and 560 nm (lower).

It is important to note that precise reverse contrast is not observed in all of our samples. Locations with stronger band-edge emission sometimes also show strong yellow band. Figure 4 in reference 11 is an example of the non-reversed contrast between yellow and band-edge emission. TEM analysis of samples with reverse and identical contrast in CL imaging of band-edge and yellow emission is underway to investigate whether threading dislocations are the source of yellow band.

2.2 Donor-acceptor pair (DAP) recombination

Shown in Figure 8 are the CL images taken at 385 nm (DAP recombination)¹⁰ for the cross structure and a 50 μm stripe. For the 50 μm stripe, the first group of bright lines appears at the boundaries between the plateaus and the concave profiles. They are oriented along the stripe direction. The second group appears at the boundary between the steep walls of the concave profile and its largely flat middle part (see Figure 2 for profile). For the cross, strong DAP emission appears at the boundary between plateaus and the concave profile. This implies that DAP recombination is associated with stress created by high aspect ratio in topography.

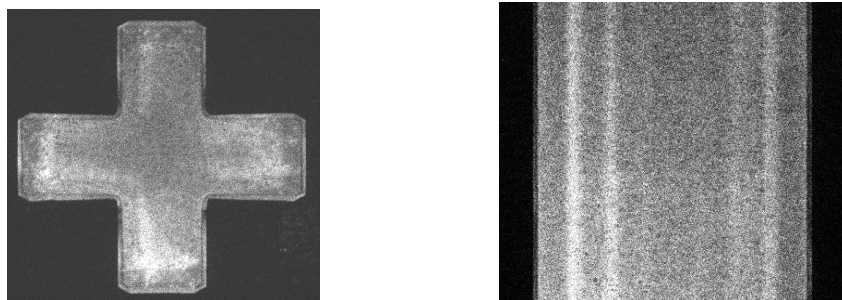


Figure 8 CL images taken at 385 nm for the cross structure (left, see Figure 3 for its SEM image) and a 50 μm stripe (topography is similar to the 75 μm stripe shown in Figure 2).

2.3 ELO of GaN: improvement of optical properties

Shown in Figure 9 are the CL images (top) and line scans (bottom) taken at 368 nm (left) and 560 nm (right) for an array of stripes with triangular cross sections, at the ELO stage before coalescence. These stripes were grown on a GaN buffer layer. Topography is similar to the one shown in Figure 5. The original stripe opening defined by lithography patterning is 5 μm and the spacing is 7 μm . For the CL distribution in the opening region, see Figure 7 and related text for discussion. It is apparent, especially from the CL line scan, that the ELO part of GaN show stronger band-edge emission (dip in the line scan is due to the gap between stripes) and weaker yellow emission than the GaN grown in the stripe opening. Similar optical characterization showing the improvement of band-edge and yellow emission through the ELO of GaN stripes with rectangular cross sections has been reported.^{18,19} In addition, we have observed the appearance of the free exciton peak in the ELO region.¹¹

Assuming the ELO region has low dislocation density as reported by other groups,⁷ the weak yellow band in the ELO region may indicate that yellow band emission is associated with dislocations. However, it could also be a result of reduced strain in the ELO material. Furthermore, point defects and impurity level in the ELO region and the vertical grown region may also be different, which could contribute to the reduction of the yellow band.

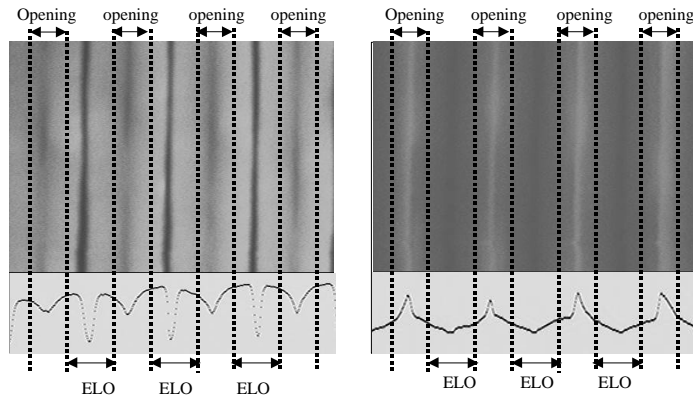


Figure 9 CL images and line scans taken at 368 nm (left) and 560 nm (right) for an array of stripes at the ELO stage before coalescence with triangular cross section.

SUMMARY

We have reported the topography evolution of GaN stripes as a function of pattern geometry, growth parameters and substrate. Wide stripes with the plateaus on both sides evolve with stripe width into flat top stripes with vertical sidewalls. Small fill factor and rough substrate favor the formation of triangular stripes. These GaN structures have been characterized by CL and implications of the spatial correlation of optical properties have been discussed.

ACKNOWLEDGEMENT

The authors wish to thank D. S. Roh and A. M. Jones for technical assistance and X. Li would like to acknowledge the support of a NSF Grant (DMR-9714289).

REFERENCES

- ¹ S. Nakamura, M. Senoh, S. Nagahama et al. *Appl. Phys. Lett.* **72**, 211 (1998).
- ² T. Nishinaga, T. Nakano and S. Zhang, *Jpn. J. Appl. Phys.* **27**, L964 (1988).
- ³ S. Naritsuka and T. Nishinaga, *J. Cryst. Growth* **174**, 622 (1997).
- ⁴ T. Tanaka, K. Uchida, A. Watanabe, and S. Minagawa, *Appl. Phys. Lett.* **68**, 976 (1996).
- ⁵ T. Akasaka, Y. Kobayashi, S. Ando, and N. Kabayashi, *Appl. Phys. Lett.* **71**, 2196 (1997).
- ⁶ D. Kapolnek, S. Keller, R. Vetury, R. D. Underwood, P. Kozodoy, S. P. Den Baars, and U. K. Mishra, *Appl. Phys. Lett.* **71**, 1204 (1997).
- ⁷ O. Nam, M. D. Bremser, T. S. Zheleva, and R. F. Davis, *Appl. Phys. Lett.* **71**, 2472 (1997) and T. S. Zheleva, O. Nam, M. D. Bremser, and R. F. Davis, *Appl. Phys. Lett.* **71**, 2638 (1997).
- ⁸ Y. Kato, S. Kitamura, K. Hiramatsu, N. Sawaki, *J. Cryst. Growth* **144**, 133 (1994).
- ⁹ A. Usui, H. Sunakawa, A. Sakai and A. A. Yamaguchi, *Jpn. J. Appl. Phys.* **36**, L899 (1997).
- ¹⁰ X. Li, A. M. Jones, S. D. Roh, D. A. Turnbull, S. G. Bishop, and J. J. Coleman, *J. Electron. Mater.* **26**, 306 (1997). X. Li, A. M. Jones, S. D. Roh, D. A. Turnbull, E. E. Reuter, S. Q. Gu, S. G. Bishop, and J. J. Coleman, *Mater. Res. Soc. Sym. Proc.* **395**, 943 (1996).
- ¹¹ X. Li, S. G. Bishop and J. J. Coleman, *Appl. Phys. Lett.* **73**, 1179 (1998).
- ¹² X. Li and J. J. Coleman, *Appl. Phys. Lett.* **70**, 438 (1997).
- ¹³ J. Park, P. A. Grudowski, C. J. Eiting, and R. D. Dupuis, *Appl. Phys. Lett.* **73**(3), 333 (1998).
- ¹⁴ O. Nam, T. S. Zheleva, M. D. Bremser, and R. F. Davis, *J. Electron. Mater.* **27**, 233 (1998).
- ¹⁵ H. Marchand, preprints.
- ¹⁶ S. J. Rosner, E. C. Carr, M. J. Ludowise, G. Girolami, H. I. Erikson, *Appl. Phys. Lett.* **70**, 420 (1997).
- ¹⁷ F. A. Ponce, D. P. Bour, W. Gotz, P. J. Wright, *Appl. Phys. Lett.* **68**, 57 (1996).
- ¹⁸ J. A. Freitas, Jr., O. Nam, R. F. Davis, G. V. Saparin, and S. K. Obyden, *Appl. Phys. Lett.* **72**, 2990 (1998).
- ¹⁹ Z. Yu, M.A.L. Johnson, T. McNulty, J.D. Brown, J.W. Cook, Jr, J.F. Schetzina, *MRS Internet J. Nitride Semicond. Res.* **3**, 6(1998).